Investigations on Nanoparticle−Chromophore and Interchromophore Interactions in Pyrene-Capped Gold Nanoparticles

Binil Itty Ipe and K. George Thomas*

Photosciences and Photonics Division, Regional Research Laboratory (CSIR), Trivandrum 695 019, India

Received: April 17, 2004; In Final Form: June 11, 2004

Three pyrene alkanethiol derivatives (**P1**, **P2**, and **P3**) possessing flexible alkyl groups of different lengths were attached to nanoparticles of gold (∼2−3 nm in size) along with dodecanethiol (Au−**P1**, Au−**P2**, and Au−**P3**). The photophysical properties of these systems were investigated as a function of (i) distance of chromophore from gold core, (ii) concentration of pyrene on gold surface, and (iii) solvent polarity. The structured absorption bands of the pyrene chromophore were significantly perturbed near the surface of gold nanoparticles (Au−**P1**), indicating a strong ground state interaction between the plasmon electrons of Au nanoparticles and the π-electron cloud of the chromophore. Such effects were not observed in Au−**P2** and Au−**P3** systems, in which the linker groups are long enough to prevent any ground state interactions. A gradual increase in the peak intensity ratio of band III/I of the normal fluorescence of pyrene chromophore was found with an increase in length of the spacer group. These results indicate that the local environment close to the surface of the Au nanoparticle is more polar compared to the bulk medium. Interchromophoric interactions are limited in the Au−**P1** system due to the restriction imposed by the curvature of spherical gold nanoparticle whereas the flexible alkyl chain tethering pyrene in Au−**P2**/Au−**P3** allows free interaction between chromophores. Steady state and time-resolved emission studies indicate that the normal fluorescence and intermolecular excimer formation are the main deactivation channels of the singlet excited state of pyrene linked to Au nanoparticles, in nonpolar solvents. In contrast, the competitive electron transfer to the gold nanocore dominates in polar solvents.

Introduction

Metal hybrids of chromophores assembled as two- or three-dimensional assemblies provide routes for hybrid materials with novel optical, electrical, and photochemical properties.[1−8] Most of the earlier studies on the interaction between fluorophores and metals are limited to bulk gold surfaces, modified with self-assembled monolayers.[9] A total quenching of the singlet excited state is observed in these systems due to the efficient overlap of orbitals.[10] In contrast, recent studies on the photophysical properties of chromophore linked gold nanoparticles have suggested a dramatic suppression in the quenching of the singlet excited state when these chromophores are densely packed on Au nanoparticles.[11−14] A better understanding of various excited state processes in chromophore functionalized metal nanostructures facilitate the effective utilization of such systems as optoelectronic devices (sensors, switches, light harvesting systems) and biological probes. For investigating the excited state interactions between chromophores and gold nanoparticles, we have selected a polycyclic aromatic hydrocarbon, namely, pyrene.

Unlike other aromatic compounds, pyrene-based molecular systems have proved to be a versatile class of probe molecule in both chemistry and biology.[15] Pyrene and its derivatives, in the monomeric form, show structured absorption and emission peaks, which are extremely sensitive to their environments.[15,16] For example, the S_0-S_1 band of pyrene is symmetry forbidden and is weak, which shows a marked intensity enhancement in polar solvents (Ham effect), providing information on the polarity of the local environment.[17] Pyrene-based chromophores show broad excimer emission with an increase in concentration and exciplex emission in the presence of electron donors.[18,19] Also, pyrene-based molecular systems can act as electron donors or acceptors in photoinduced processes.[18,19] In a recent communication, we have reported the spectroscopic evidence for an electron transfer process from the pyrene chromophore to gold nanoparticle, on laser excitation.[11] The present report deals with detailed spectroscopic characterization of pyrene functionalized on Au nanoparticles, by varying (i) solvent polarity, (ii) distance of chromophore from gold core, and (iii) loading of pyrene on gold nanoparticle surface. Pyrene alkanethiols possessing alkyl groups of different chain lengths (**P1**, **P2**, **P3**) were selected for this purpose (Chart 1). These chromophores were functionalized onto Au nanoparticles (Au−**P1**, Au−**P2**, and Au−**P3**) by co-binding with dodecanethiol in different molar ratios.

Results and Discussion

Synthesis and Characterization. Synthesis of **P1**, **P2**, and **P3** was carried out as per Scheme 1. The bromoalkyl pyrene derivatives (**3a** and **3b**) were prepared through a nucleophilic substitution reaction of 1-pyrenemethanol with the corresponding α,ω-dibromoalkanes, using sodium hydride as base. The corresponding bromo derivatives were converted to the thiols (**P1**, **P2**, and **P3**) using a method reported by Fox and co-workers,[20] and by reacting with a mixture of tetrabutylammonium fluoride and hexamethyldisilathiane. Details of the synthesis and characterization of various intermediates and thiol derivatives of pyrene (**P1**, **P2**, and **P3**) are given in the Experimental Section.

* To whom correspondence should be addressed. E-mail: georgetk@md3.vsnl.net.in.

10.1021/jp048321a CCC: $27.50
Published on Web 08/06/2004

CHART 1: Pyrene Alkanethiols Used To Functionalize Gold Nanoparticles

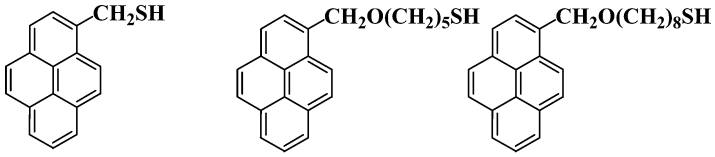

SCHEME 1: (a) PBr_3, $CHCl_3$; (b) $Br(CH_2)_nBr$, NaH, THF, Reflux; (c) Hexamethyldisilathiane, Tetrabutylammonium Fluoride, THF, −10 °C

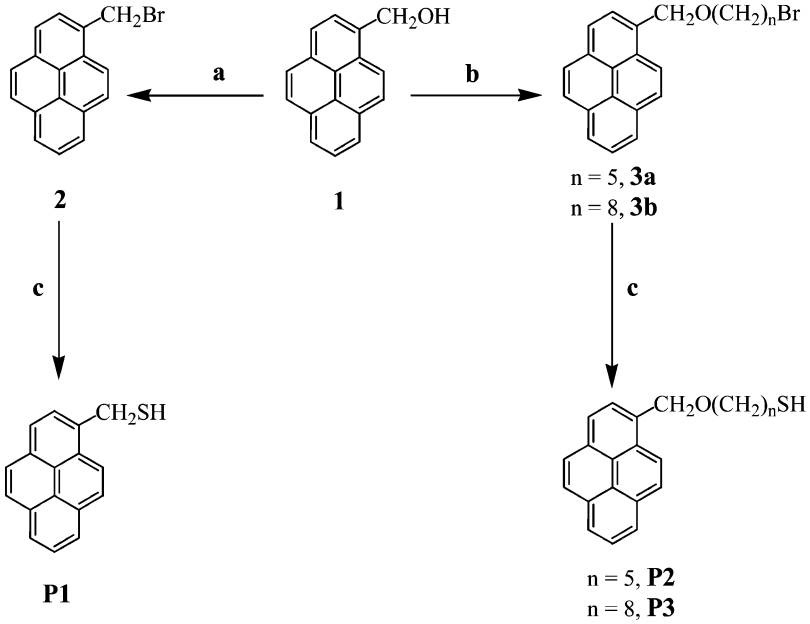

Synthesis and Characterization of Pyrene-Capped Gold Nanoparticles. Pyrene chromophores, **P1**, **P2**, and **P3**, were functionalized on Au nanoparticles by adopting a biphasic synthetic procedure similar to that reported by Brust et al.[21] Gold nanoparticles were functionalized with the corresponding pyrene derivative and dodecanethiol in different molar ratios (3:17, 3:7, 3:2). In a typical preparation of dodecanethiol/**P2** functionalized gold nanoparticles, an aqueous solution of hydrogen tetrachloroaurate(III) hydrate (50 μmol in 2 mL) was stirred with tetraoctylammonium bromide (250 μmol in 5 mL of toluene) for 5 min, until all the aurate ions were transferred into the toluene layer. To this was added a solution of dodecanethiol and **P2**, in the molar ratio 2:3 (metal to thiol molar ratio was kept as 1:1) in 2 mL of THF. After stirring for 2−3 min, sodium borohydride (2.5 mmol in 2 mL of water) was added and the mixture was stirred for 3 h. The hybrid nanoparticles formed were purified by repeated precipitation and filtration using ethanol (3 × 100 mL). The brown powder obtained was redispersed in toluene.

Various methods adopted for the characterization of monolayer-protected clusters of gold nanoparticles have been reviewed recently by Murray and co-workers.[3] Specific examples of characterization of monolayer-protected gold clusters have also been reported, which includes alkenethiolate,[22] arenethiolate,[23] alkylstilbenethiolate,[24] and ω-fluorenyl-alkene-1-thiolate.[13] In the present case pyrene-capped Au nanoparticles were characterized using High-Resolution Transmission Electron Microscopy (HRTEM), FTIR and ^{1}H NMR spectroscopy. The HRTEM image of Au nanoparticle functionalized with **P2** is presented in Figure 1. Samples were prepared by drop casting the nanoparticle suspension onto a carbon-coated copper grid.

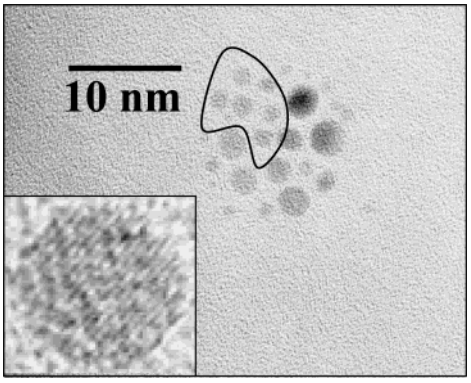

Figure 1. TEM images of gold nanoparticles functionalized with **P2** after drop casting onto a carbon-coated copper grid. Inset shows the HRTEM of Au−**P2**.

Relatively dilute suspension of Au nanoparticle were used to prevent the possibility of aggregation of nanoparticles. Images presented in Figure 1 indicate the presence of two types of clusters; smaller gold nanoparticles with an average size of 2.2 nm (clusters in the highlighted area of Figure 1) and larger clusters with a size ∼3.0 nm. The lattice planes observed in the HRTEM image of the nanoparticle (inset of Figure 1) indicate that the nanoparticles are crystalline in nature. The larger clusters (∼3.0 nm) observed on the grid may be formed as a result of the interparticle aggregation of smaller particles. On the other hand, interparticle clustering is not observed for pyrene-capped nanoparticles when suspended in various organic solvents, and this was established by various spectroscopic methods in later sections. It was reported earlier that the size of the ligand is one of the factors that influences the size of

SCHEME 2: Schematic Representation of the Functionalization of Au Nanoparticles with Different Concentrations of Pyrene Alkanethiol

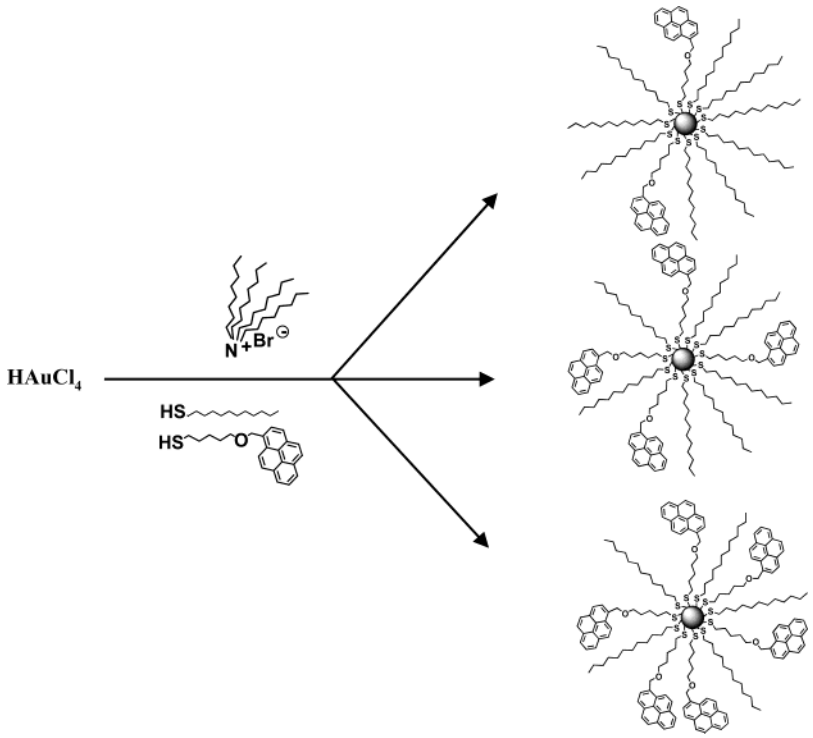

nanoparticles during its formation. For example, arenethiolate-stabilized gold nanoparticles possesses a larger size than alkanethiolate-stabilized gold nanoparticles.[23] In the present case, the average size of gold nanoparticles functionalized with **P2** is similar to that of alkanethiol-protected clusters. This may be due to the fact that the bulky pyrenyl chromophores in Au−**P2** are well separated from the gold core by means of the methylene chains and hence may not influence the size of the particle.

The present study mainly deals with chromophore−nanoparticle interaction and interchromophore interaction on the surface of a nanoparticle and the average number of photoactive molecules per nanoparticle plays a decisive role in tuning the photophysical properties. Co-binding alkanethiols with thiol derivatives of pyrene molecules (**P1**, **P2**, **P3**), in different proportions, enabled us to fix the desired number of photoactive molecules around the Au nanoparticles. A schematic representation of the functionalization of Au nanoparticles with pyrene derivatives and dodecanethiol, in different molar ratios, is presented in Scheme 2. It may be noted that it is difficult to estimate the exact concentration of dodecanethiol bound onto a Au nanoparticle. The average diameter of a Au nanoparticle is 2.2 nm, and on this basis, we have estimated the number of gold atoms as 323, similar to that reported by Fox and co-workers.[13] The estimations were carried out by adopting a tight-packed spherical model suggested by Murray and co-workers, which assigns the gold core as a sphere with density of 58.01 atoms/nm^3 covered with a skin of hexagonally close-packed gold atoms with number density of surface gold atoms as 13.89 atoms/nm^2.[25]

The average number of **P2** molecules per nanoparticle was varied by co-binding **P2** and dodecanethiol in the molar ratios of 3:17, 3:7, and 3:2. The concentration of unreacted **P2**, in each case, was estimated from UV−vis absorption spectrum of the filtrate. For estimating the number of pyrene chromophores attached on single gold nanoparticle, we have assumed that all gold ions are converted to nanoparticles and pyrene alkanethiols are evenly distributed on the surface of nanoparticles suspended in the solution. It is estimated that approximately 30, 45, and 55 chromophores are attached on each nanoparticle by functionalizing **P2** and dodecanethiol in the molar ratios of 3:17, 3:7, and 3:2 (details of estimation are given as Supporting Information). Thus, we have varied the number of pyrene molecules attached to the surface of a gold nanoparticle and it may be more meaningful to represent it as the local concentration of chromophore.

The radius and volume of pyrene-functionalized Au nanoparticles were calculated from theoretical calculations using Spartan software (Supporting Information). In the case of the Au−**P1** system, the pyrene molecules could be tilted onto the gold surface, making the estimation of the molecular area difficult; hence the estimation of local concentrations of chromophore was confined to the Au−**P2** system. We have considered the Au core and the organic shell, consisting of dodecanethiol and **P2**, as one unit, and the total volume is calculated from the combined radius of the gold core and shell assuming spherical symmetry. The local pyrene concentration of the Au nanoparticle system functionalized with **P2** and dodecanethiol in the molar ratios of 3:17 is estimated as 0.8 M, 3:7 as 1.2 M, 3:2 as 1.4 M (error range is less than 20% in all the cases). Details of the calculations are given as Supporting Information.

To confirm the surface functionalization of pyrene chromophore on gold nanoparticles, the ^{1}H NMR spectrum was compared with those of the corresponding pyrene alkanethiol. A representative example is shown in Figure 2. The usefulness of NMR spectroscopy in characterizing surface interactions of organic molecules on Au nanoparticles has been demonstrated.[26] In the present case a significant broadening of the NMR resonance peaks (for example, α-methylene group) was observed for **P2** on the surface of gold nanoparticles when compared to free thiolates. One of the factors contributing to the peak broadening is the dipolar spin relaxation of **P2** on the densely

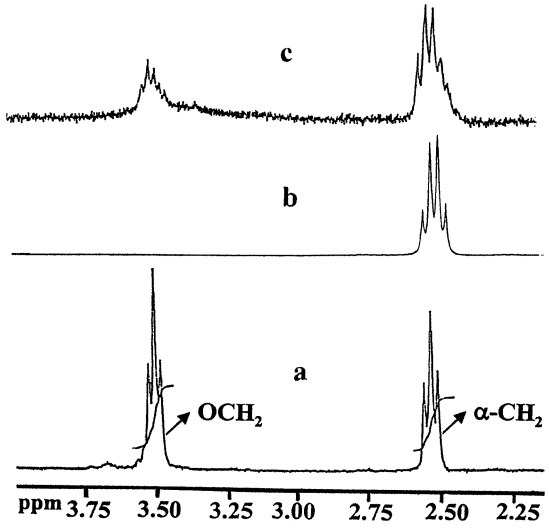

Figure 2. ^{1}H NMR spectra (δ 2.25−3.75) of (a) **P2**, (b) dodecanethiol, and (c) a mixture of **P2** and dodecanethiol (3:2) on the surface of gold clusters in $CDCl_3$.

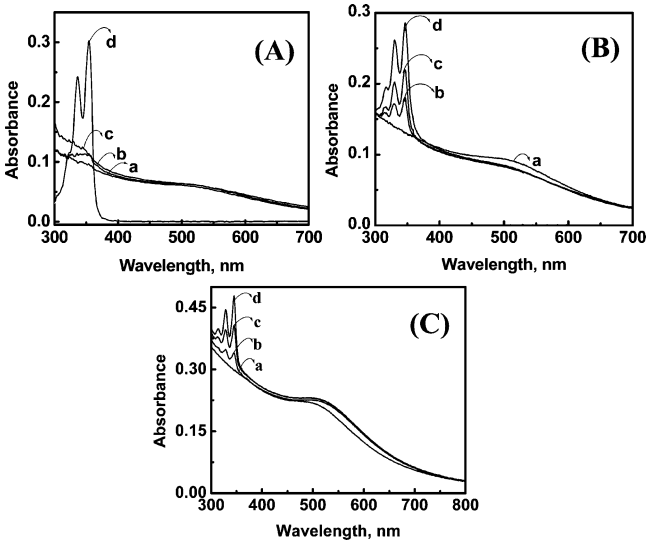

Figure 3. Absorption spectra (in toluene) of Au nanoparticles functionalized with dodecanethiol (trace a in B and C) and a mixture of pyrene alkanethiol and dodecanethiol, in different molar ratios: (A for **P1**) (a) 3:17, (b) 3:7, (c) 3:2, (d) unbound **P1**; (B for **P2**) (b) 3:17, (c) 3:7, (d) 3:2; (C for **P3**) (b) 3:17, (c) 3:7, (d) 3:2.

packed regions near the thiolate/gold interface.[3,27] It may be noted that the surface of gold nanoparticles is not uniform and the differences in the binding sites for **P2** on Au nanoparticles lead to peak broadening. Thus, the heterogeneity arising from (i) the nonuniform distribution of thiolate ligands on Au nanoparticle surface and (ii) dipolar spin relaxation, contribute to the broadening of NMR resonance peaks of the thiolates on Au nanoparticle surface.

The FTIR spectra of the unbound pyrene alkanethiols and pyrenethiolate-capped Au nanoparticles (Supporting Information) are quite similar, which indicates that the chromophores are an integral part of the nanoparticles, thereby confirming surface functionalization.[21] The aromatic C−H stretching which appears as a weak band around 3050 cm^{-1} and the aromatic C═C stretching bands between 1400 and 1600 cm^{-1} are slightly at higher energies when pyrene molecules are functionalized on gold nanoparticle.[23]

Absorption Spectral Properties. Absorption spectra of pyrene-capped Au nanoparticles (Au−**P1**, Au−**P2**, and Au−**P3**) normalized at 520 nm, with different loadings of pyrene are presented in Figure 3.

Absorption spectrum of all the three systems possesses a broad band in the visible region, which is attributed to the surface plasmon absorption of Au nanoparticles. The surface plasmon absorption originates from the interaction of external electromagnetic radiation with highly polarizable Au $5d^{10}$ electrons of Au nanoparticles.[28,29] In the present case, a significant dampening and broadening of surface plasmon absorption was observed. Such dampening is characteristic of thiolate-capped Au nanoparticles.[28,30]

Pyrene alkanethiols possess structured absorption bands and their absorption spectral features were compared with pyrene-capped Au nanoparticles possessing different loadings of chromophore. The structured absorption bands of the pyrene chromophore were found to be significantly perturbed in the case of **P1** (pyrene methanethiol), when functionalized onto the surface of gold nanoparticles (traces a−c), indicating a strong ground state interaction between the plasmon electrons of Au nanoparticles and the π-electron cloud of pyrene chromophore. The absorption characteristics of **P2** and **P3** functionalized gold nanoparticles holding different concentrations of pyrene chromophores are presented in Figures 3B and 3C (traces b−d). Interestingly, the absorption spectra of **P2**- and **P3**-capped gold nanoparticles are almost an additive spectrum of dodecanethiol-capped gold and pyrene alkanethiols of respective loadings. The structured absorption bands of pyrene chromophore observed at 313, 328, and 345 nm for **P2** and **P3** remain more or less unperturbed (traces b−d) when functionalized on Au nanoparticles. The flexible methylene spacers in **P2** and **P3** are long enough to prevent any ground state interaction between pyrene and gold nanocore in Au−**P2** and Au−**P3**. Also, the possibility of different conformers directly interacting with gold is much less due to the densely packed alkyl chains on Au nanoparticles. On the other hand, the pyrenyl moiety on Au−**P1** is very close to the metal surface and the possibility of electronic perturbation in the ground state is very high. In an earlier study, Thomas and Kamat reported the ground state interaction between 1-pyrenemethylamine (Py-CH_2NH_2) and tetraoctylammonium bromide (TOAB)-stabilized gold nanoparticles.[31]

Emission Spectral Properties. The typical changes in the intensities of the structured fluorescence bands of the monomer form of pyrene, particularly the ratio of peak III to I intensities have been extensively used as a measure of the local polarity in microheterogeneous systems.[17] The emission spectral properties of pyrene alkanethiols functionalized on Au nanoparticles with different loadings are compared in Figure 4. The peak intensity of the normal fluorescence band III of pyrene chromophore observed at 387.9 nm was compared with the band I at 379.9 nm as a function of length of the spacer group. The main objective of this analysis was to understand the polarity of the local environment of Au nanoparticle compared to bulk solvent medium. A gradual increase in III/I peak ratio was observed with the increase in spacer group between pyrene and Au nanoparticle core. The III/I peak intensity ratio of Au−**P1**, where pyrene is linked by a single methylene spacer, is estimated as 0.89. On the other hand, the ratio of peak intensities of pyrene chromophore in Au−**P2** and Au−**P3** systems, possessing five and eight methylene spacer groups, are estimated as 0.98 and 1.18, respectively. These results indicate that the local environment close to the surface of Au nanoparticle is more polar, as compared to the bulk solvent medium.

Another interesting observation is the strong dependence of excimer emission on (i) pyrene concentration on the surface of gold nanoparticles and (ii) length of the spacer groups used to

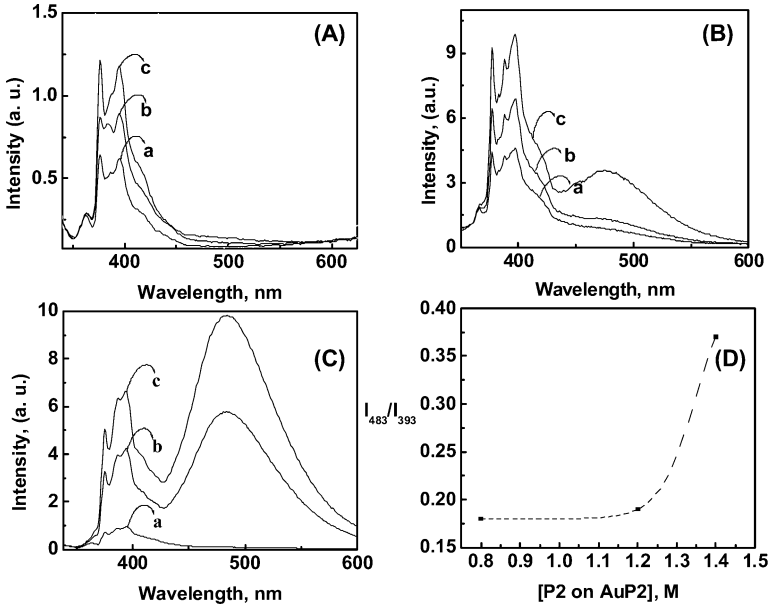

Figure 4. (A)−(C) Emission spectra (in toluene) of Au nanoparticle functionalized with a mixture of pyrene alkanethiol (**P1** in A, **P2** in B, and **P3** in C) and dodecanethiol in different molar ratios of 3:17 (a), 3:7 (b), 3:2 (c). (D) Plot of fluorescence intensity ratio of monomer to excimer as a function of concentration of **P2** on the surface of gold nanoparticles (excitation at 328 nm; Au nanoparticle concentrations were kept constant by optically matching the solutions at 520 nm).

link pyrene chromophore on to Au nanoparticle. Excimer emission is usually observed in the spectral region of 425−600 nm when the concentration of pyrene is high enough to form excited state dimers or in constrained/heterogeneous media wherein the mobility of the polynuclear aromatic hydrocarbon molecule is minimized.[16] The concentration dependence of pyrene chromophore binding to Au nanoparticle was earlier investigated by Chen and Katz by titrating Au nanoparticle with pyrene chromophore possessing thioester/thicarbonate functional group.[32,33] It is well established that the optimum condition for excimer formation in pyrene is a parallel, sandwich type aggregate with an interplanar separation of 353 pm.[16]

The intensity of the excimer fluorescence (excimer fluorescence intensity, I_E at 483 nm) of pyrene chromophore was compared with the normal fluorescence (monomer fluorescence intensity, I_M at 393 nm) for quantifying the interchromophoric mobility in the excited state. For all the three system under investigation, the I_E/I_M ratio was found to be in the range of 0.10−0.20 at low loading (trace a in Figure 4A−C). In Au−**P1** system, where pyrene chromophore is linked to the Au nanoparticle through a single methylene group**,** excimer emission is found to be weak even at higher loadings of pyrene chromophore (I_E/I_M = 0.13). This may be attributed to the limited interaction between the pyrene chromophores on the Au nanoparticle surface due to the restrictions imposed by the curvature of spherical gold nanoparticle, which results in a larger interplanar distance between the chromophores. In an earlier report, the inefficient cycloaddition between *trans*-4-(mercaptoheptoxy)stilbene on the surface of gold nanoparticles imposed by its curvature was discussed by Zhang et al.[24] The pyrene chromophores in Au−**P1** are deeply embedded inside dodecanethiol due to interdigitation that limits the mobility of chromophores. The intensity of the excimer emission band was investigated by varying the linker properties in Au−**P2** and Au−**P3** nanoassemblies, which possess five and eight methylene spacer groups between Au nanoparticle and pyrene chromophore (Figure 4B,C). A representative plot of I_E/I_M versus the concentration of **P2** is presented in Figure 4D. Interestingly, prominent excimer emission is observed at higher loadings in both these systems (trace b and c in Figure 4B,C) and this effect is more pronounced in Au−**P3** systems (for example, I_M/I_E ratio is 0.6 at higher loadings; see trace c in Figure 4C). The flexible alkyl chain tethering pyrene in Au−**P3** is sufficiently long enough to protrude outside the dodecanethiol layer allowing free interaction between pyrene molecules, at higher loadings.

Interparticle interactions may also lead to excimer emission, irrespective of the loading of pyrene chromophore, and such interactions would give rise to an interparticle plasmon coupling. This type of coupling can shift the plasmon absorption of gold nanoparticles to the red region.[34] Such a shift in plasmon absorption is not observed in the present case ruling out the possibility of excimer emission resulting through an interparticle interaction. The spectral shapes of the plasmon absorption band for a specific pyrene-capped Au nanoparticle remain more or less the same.

Time-Resolved Fluorescence Studies. From steady state experiments, it is difficult to evaluate the quantum yield of fluorescence of pyrene chromophores functionalized on gold nanoparticle due to the spectral overlap of the plasmon absorption of the nanoparticle. The fate of the singlet excited state of pyrene functionalized on Au nanoparticle was elucidated using time-resolved fluorescence studies. The decay of pyrene chromophore when attached to another molecular component is often multiexponential.[35,36] In the present case, the possible deactivation pathways of the singlet excited state of pyrene functionalized on Au nanoparticle were investigated from their singlet lifetimes by varying the (i) length of the alkyl chain, (ii) loading of the chromophores on Au nanoparticle, and (iii) solvent polarity. Fluorescence lifetimes were measured from the fluorescence decay of **P1**, **P2**, and **P3** and the corresponding pyrene alkanethiol capped on gold nanoparticles using a picosecond single photon counting system. The details of the instrumental setup are presented in the Experimental Section. In all these experiments, the solutions were thoroughly degassed by purging with argon. The samples were excited at 360 nm and the emission collected at 390 nm to evaluate the decay of the singlet-excited state of the monomer whereas the excimer emission (consisting of the growth component and decay component) was monitored at 500 nm.

TABLE 1: Fluorescence Lifetimes[a−c] and Fractional Contributions[d] of Pyrene Alkanethiols (P1, P2, and P3) in Toluene

	fluorescence lifetimes					
	decay at 390 nm			growth at 500 nm	decay at 500 nm	
system	τ_1, ns (χ_1%)	τ_2, ns (χ_2%)	χ^2	τ_1, ns	τ_2, ns	χ^2
P1	8.6 (81%)	1.8 (19%)	1.10	1.8	8.5	1.10
P2	7.9 (65%)	2.5 (35%)	1.10	2.5	28.1	1.10
P3	7.6 (71%)	2.5 (29%)	1.05	2.5	11.5	1.06

[a] τ_1 and τ_2. [b] Error limit ±5%. [c] Excited at 360 nm. [d] χ_1 and χ_2.

Unbound pyrene alkanethiols, **P1**, **P2**, and **P3** follow biexponential decay, with long-lived and short-lived components. The long-lived component at 390 nm ($\tau_1 \sim 8$ ns, Table 1) is attributed to the inherent lifetime of pyrene alkanethiol. The short-lived species ($\tau_2 = 1.8-2.5$ ns, Table 1) is assigned to the decay of quenched pyrene alkanethiol molecules, resulting from the interaction with another ground state pyrene alkanethiol molecule, leading to the formation of excited state dimers. On the basis of steady state emission studies, the band at 500 nm is attributed to the excimer emission, and their intermolecular interactions were investigated in detail using time-resolved fluorescence studies. The trace at 500 nm consist of a growth component corresponding to the formation of pyrene excimer and another long-lived decay component corresponding to the decay of excimer which were fitted together. The growth corresponding to the formation of excimer has a rise time of 1.8−2.5 ns. The formation of excimer is a dynamic process resulting from the interchromophoric interaction between an excited state pyrene chromophore and a ground state pyrene. This is supported by the fact that the decay kinetics of the short-lived component at 390 nm (~2 ns) matches well with the rise time of the excimer at 500 nm (Table 1). The long-lived component at 500 nm corresponds to the intrinsic decay time of pyrene excimer. The singlet lifetime of pyrene alkanethiols (**P1**, **P2**, **P3**) were investigated in solvents of varying polarity and the results are presented under Supporting Information. In all solvent systems that we have investigated, the decay of the unbound pyrene alkanethiols at 390 nm follows a biexponential decay. The lifetimes of the long-lived (τ_1) as well as short-lived (τ_2) species and their fractional contributions remain more or less unaffected ruling out the possibility of excited state deactivation through other channels.

The decay characteristics of pyrene derivatives, **P1**, **P2**, and **P3** when bound to the surface of gold nanoparticles were further investigated in a nonpolar solvent such as toluene and the results are presented in Table 2. The lifetimes of the long-lived (τ_1) and short-lived (τ_2) components and their relative distribution remain more or less unaffected in toluene when **P3** is functionalized on Au nanoparticles, ruling out the possibility of any quenching process (electron or energy transfer). On the other hand, an additional species, with extremely short lifetime (τ_3) was observed along with the long-lived (τ_1) and short-lived (τ_2) species, when **P1** and **P2** are attached on gold nanoparticles (τ_3 = 27 ps (15%) for Au−**P1**, τ_3 = 48 ps (10%) for Au−**P2**).

To study the quenching mechanism of pyrene on the surface of gold nanoparticles, in detail, we have carried out the time-resolved lifetime studies as a function of (i) solvent polarity (Table 3) and (ii) concentration of pyrene alkanethiol on Au surface (Table 4). In polar solvents, photoinduced electron transfer process is thermodynamically more favorable and we have investigated the effect of solvent polarity on the relative amplitude of various decay components. Interestingly, an additional short-lived species was observed in all the three cases (Table 3 and Supporting Information) in polar solvents. It is observed that the relative abundance of the short-lived species (τ_3) increases significantly with increase in solvent polarity (Table 3), further confirming the light-induced electron transfer from pyrene chromophore to the gold nanocore. The mechanism of quenching and the formation of radical cation was earlier established in the case of Au−**P2** by following laser flash photolysis.[11] Pulsed laser irradiation (337 nm) of the Au−**P2** nanoparticle, in polar solvents such as tetrahydrofuran, resulted in transfer of an electron from pyrene to gold nanoparticle.

The possibility of fast decay of the singlet excited state of pyrene in a polar solvent by a self-quenching process, through interactions between pyrene chromophores bound on Au nanoparticles, is further ruled out by varying the concentration of chromophore on Au nanoparticle. A self-quenching process would imply that the relative amplitude of the quenched species should increase with increased concentration of pyrene on nanoparticles. It is observed that the lifetimes as well as the relative amplitude of all the three components are independent of the concentration of pyrene (Table 4) and the self-quenching pathway through interaction of adjacent pyrene is ruled out. These results clearly indicate that the quenching of the singlet excited state of pyrene bound on gold is not due to self-quenching processes but as a result of electron transfer from the singlet-excited state of pyrene to gold nanoparticles.

The excimer characteristics (growth and decay at 500 nm; Table 2) of pyrene alkanethiols bound to the surface of Au nanoparticles were similar to those of the unbound pyrene alkanethiols (Table 1). The trace at 500 nm for Au−**P2** and Au−**P3** has a rise time (τ_1) resulting from the formation of excimer. The long-lived decay component (τ_2) may be attributed to the decay of the excimer and the short-lived decay component (τ_3) may be attributed to the quenched excimer species.

Thus, the main deactivation channels of the singlet excited state of pyrene linked on Au nanoparticles are (a) normal fluorescence, (b) intermolecular excimer formation and (c) the competitive electron transfer to the gold nanocore. The first two processes are favorable in nonpolar solvents whereas the latter one dominates in polar solvents.

Conclusions

Pyrene chromophores functionalized to gold nanoparticles using methylene groups of varying chain length were prepared. The nanoparticle−chromophore and interchromophore interactions were investigated in detail. On the basis of emission spectral studies, it is concluded that the local environment close to the surface of Au nanopartcle is more polar compared to the bulk medium. The flexible linker provides a topographical control on the various interactions leading to the formation of excimers at higher loadings. The suppression in the quenching of the singlet-excited state of **P3** (long alkyl chain tethered pyrene chromophore) on the surface of gold, when compared to **P1** and **P2** could be further extended for the development of photocatalysts as well as chemical and biological sensors. Time-resolved fluorescence studies indicate that the photoinduced electron transfer process from pyrene to the Au core is favored in polar solvents. In summary, it is possible to modulate the ground as well as excited state interactions, particularly the quenching of the singlet excited state of the chromophore, by systematically varying the chain length of the chromophore tethering the gold nanoparticle and the concentration of the chromophore on nanoparticle surface.

TABLE 2: Fluorescence Lifetimes[a−c] and Fractional Contributions[d] of Gold Nanoparticle, Functionalized with a Mixture of Pyrene Alkanethiol and Dodecanethiol (Molar Ratio of 3:17) in Toluene

	fluorescence lifetimes							
	decay at 390 nm				growth at 500 nm	decay at 500 nm		
system	τ_1, ns (χ_1%)	τ_2, ns (χ_2%)	τ_3, ns (χ_3%)	χ^2	τ_1, ns	τ_2, ns	τ_3, ns	χ^2
Au−P1	14.8 (60%)	3.6 (25%)	0.027 (15%)	1.2	-			
Au−P2	7.96 (80%)	1.30 (10%)	0.048 (10%)	1.1	1.50	9.60	0.10	1.3
Au−P3	9.02 (90%)	1.88 (10%)	-	1.0	1.50	8.78		1.2

[a] τ_1, τ_2, and τ_3. [b] Error limit ±5%. [c] Excited at 360 nm. [d] χ_1, χ_2, and χ_2.

TABLE 3: Comparison of Fluorescence Decay Times[a−c] and Fractional Contributions[d] of Au−P2 as a Function of Solvent Polarity

	fluorescence lifetimes of Au−P2 in different solvents			
solvent	τ_1, ns (χ_1%)	τ_2, ns (χ_2%)	τ_3, ns (χ_3%)	χ^2
toluene	8.1 (64)	1.3 (22)	0.048 (14)	1.3
dichloromethane	10 (23)	1.1 (5)	0.016 (72)	1.08
acetone	*e*		*f*	
acetonitrile	*e*		*f*	

[a] τ_1, τ_2, and τ_3. [b] Error limit ±5%;. [c] Excited at 36 nm. [d] χ_1, χ_2, and χ_2. [e] Long-lived component is absent. [f] The short-lived species is the major component and it is difficult to measure the lifetime because it is close to the instrument response time.

TABLE 4: Comparison of Fluorescence Decay Times[a−c] and Fractional Contributions[d] of Au−P2 as a Function of P2 Loading

percentage of **P2**	τ_1, ns (χ_1%)	τ_2, ns (χ_2%)	τ_3, ns (χ_3%)	χ^2
15	9.6 (28)	1.2 (4)	0.013 (68)	1.10
30	8.7 (28)	0.64(3)	0.022 (69)	1.13
70	10 (23)	1.1(5)	0.016 (72)	1.08

[a] $\tau_1$and τ_2. [b] Error limit ± 5%. [c] Excited at 360 nm. [d] χ_1 and χ_2.

Experimental Section

Materials and Instrumental Techniques. Solvents and reagents used were purified and dried by standard methods. All starting materials and reagents were purchased from Sigma-Aldrich and were used as such. Photophysical studies were carried out using spectroscopic grade solvents. All melting points were determined with a Mel-Temp-II melting point apparatus and are uncorrected. ^{1}H and ^{13}C NMR spectra were measured on a 300 MHz Bruker Advance DPX spectrometer. IR spectra were recorded on a Nicolet Impact 400D infrared spectrophotometer. Emission spectra were recorded on a SPECTRACQ spectrofluorometer and corrected using the program supplied by the manufacturer. The electronic absorption spectra were recorded on a Shimadzu Model UV-3101 PC UV−vis−NIR scanning spectrophotometer. For TEM studies, a drop of colloidal gold solution was placed on a carbon-coated copper grid and the solvent was allowed to evaporate. Specimens were examined on a Hitachi H600 transmission electron microscope.

Fluorescence lifetimes were measured using a Tsunami Spectra Physics single photon counting system. Ti sapphire laser, having a fundamental wavelength of 934 nm, was used as the excitation source. The average output power is 680 mW with a pump power of 4.5 W. The pulse width of the laser is <2 ps. The flexible harmonic generator (FHG) gives the second harmonic (467 nm) output from the Tsunami laser system. The fluorescence was detected using a two-stage microchannel plate photomultiplier (MCP-PMT R38094). The fluorescence decay measurements were further analyzed using the IBH software library, which includes an iterative shift of the fitted function as part of χ^2 goodness of the fit criterion.

Synthesis of 1-(1-Pyrenyl)-1-bromomethane, 2. To a solution of 1-pyrenemethanol (250 mg, 1.07 mmol) in dry dichloromethane (20 mL) kept in an ice-bath was added PBr_3 dropwise with stirring. The reaction mixture was stirred for 12 h and then neutralized with sodium bicarbonate solution. The organic layer was extracted with dichloromethane and concentrated to give **2** (317 mg, 1.07 mmol) in nearly quantitative yield, mp 136−137 °C. IR (KBr), ν_{max}: 2952, 1920, 1649, 1593, 1434, 1177, 1181, 1065 cm^{-1}. ^{1}H NMR (300 MHz, $CDCl_3$): δ 5.25 (2H, s, $ArCH_2$), 8.00−8.39 (9H, m, aromatic) ppm. ^{13}C NMR (75 MHz, $CDCl_3$): δ 32.15, 122.78, 124.81, 125.59, 126.23, 127.29, 127.66, 127.99, 128.20 ppm.

Synthesis of 1-(1-Pyrenyl)-1-methanethiol, P1. To a stirred solution of **2** (200 mg, 0.64 mmol) in distilled THF (10 mL), kept at −10 °C, were added hexamethyldisilathiane (137.6 mg, 0.96 mmol) and 1 mL (1 mmol) of terabutylammonium fluoride from a 1 M stock solution in THF containing 5% water. The reaction mixture was stirred for 12 h and then diluted with dichloromethane. The organic layer was washed with saturated ammonium chloride solution, and the solvent was removed under reduced pressure. The product was precipitated by adding hexane to give 98 mg (60%) of **P1**, mp 164 °C. IR (KBr), ν_{max}: 2941, 2868, 1142, 850, 724 cm^{-1}. ^{1}H NMR (300 MHz, $CDCl_3$): δ 4.2 (2H, s, $ArCH_2$−SH), 7.96−8.39 (9H, m, aromatic) ppm. ^{13}C NMR (75 MHz, $CDCl_3$): δ 26.89, 122.78, 124.81, 125.59, 126.23, 127.29, 127.66, 127.99, 128.20 ppm. Exact mass calculated 248.0660, (M^+) found 248.0579 (EI^+ high-resolution mass spectroscopy).

Synthesis of 1-(1-Pyrenyl)-2-oxo-7-bromoheptane, 3a. To a suspension of sodium hydride (200 mg, 0.8 mmol) in dry THF (10 mL) were added 1-pyrenemethanol (200 mg, 0.8 mmol) and 1,5-dibromopentane (1 g, 4 mmol) in dry THF (25 mL) dropwise over a period of 30 min. The reaction mixture was refluxed for 20 h. On cooling, the reaction mixture was quenched with cold water and the organic layer was extracted with dichloromethane. The solvent was removed under reduced pressure, and the product was recrystallized from a mixture (1:5) of ethyl acetate and hexane, to give 185 mg (85%) of **3a**, mp 81 °C. IR (KBr), ν_{max}: 2950, 1920, 1647, 1593, 1434, 1181, 1065 cm^{-1}. ^{1}H NMR (300 MHz, $CDCl_3$): δ 1.5−1.8 (6H, m, alkyl), 3.3−3.8 (2 H, t, CH_2Br), 3.5−3.6 (2H, t, OCH_2), 5.2 (2H, s, $ArCH_2$), 7.9−8.3 (9H, m, aromatic) ppm. ^{13}C NMR (75 MHz, $CDCl_3$): δ 24.96, 28.96, 32.52, 33.72, 70.07, 71.57, 76.56, 123.44, 124.46, 125.18, 125.90, 126.90, 127.36, 127.64, 129.32, 130.80, 131.23, 131.59 ppm. Exact mass calculated 381.0854, ($M^{\bullet+}$) found 381.0860 (FAB high-resolution mass spectroscopy).

Synthesis of 1-(1-Pyrenyl)-2-oxoheptanethiol, P2. To a stirred solution of **3a** (500 mg, 1.31 mmol) in distilled THF (10 mL), kept at −10 °C, were added hexamethyldisilathiane (280 mg, 1.57 mmol) and 1.5 mL (1.5 mmol) of terabutylammonium fluoride from a 1 M stock solution in THF containing 5% water. The reaction mixture was stirred for 12 h and then diluted with dichloromethane. The organic layer was washed

with saturated ammonium chloride solution, and the solvent was removed under reduced pressure. The product was precipitated by adding hexane to give 400 mg (82%) of **P2**, mp 88 °C. IR (KBr), ν_{max}: 2941, 2868, 1142, 850, 724 cm^{-1}. ^1H NMR (300 MHz, $CDCl_3$): δ 1.44−1.67 (6H, m, alkyl), 2.56−2.61 (2H, t, CH_2S), 3.55−3.59 (2H, t, OCH_2), 5.18 (2H, s, $ArCH_2$), 7.96−8.35 (9H, m, aromatic) ppm. ^{13}C NMR (75 MHz, $CDCl_3$): δ 24.96, 28.96, 32.52, 33.72, 70.07, 71.57, 123.44, 124.46, 125.18, 125.90, 126.90, 127.36, 127.64, 129.32, 130.80, 131.23, 131.59 ppm. Exact mass calculated 334.1391, ($M^{\bullet+}$) found 334.1385 (FAB high-resolution mass spectroscopy).

Synthesis of 1-(1-Pyrenyl)-2-oxo-10-bromodecane, 3b. To a suspension of sodium hydride (516 mg, 21.5 mmol) in dry THF (10 mL) were added 1-pyrenemethanol (500 mg, 2.15 mmol) and 1,8-dibromopentane (3 g, 10.75 mmol) in dry THF (25 mL) dropwise over a period of 30 min. The reaction mixture was refluxed for 20 h. On cooling, the reaction mixture was quenched with cold water and the organic layer was extracted with dichloromethane. The solvent was removed under reduced pressure, and the product was recrystallized from a mixture (1:5) of ethyl acetate and hexane, to give 636 mg (70%) of **3b**, mp 45 °C. IR (KBr), ν_{max}: 2951, 1923, 1645, 1591, 1434, 1180, 1065 cm^{-1}. ^1H NMR (300 MHz, $CDCl_3$): δ 0.89−1.25 (12H, m, alkyl), 3.31−3.35 (2 H, t, CH_2Br), 3.57−3.61 (2H, t, OCH_2), 5.20 (2H, s, $ArCH_2$), 7.97−8.39 (9H, m, aromatic) ppm. ^{13}C NMR (75 MHz, $CDCl_3$): δ 24.96, 28.96, 33.72, 70.07, 71.57, 76.56, 123.44, 124.46, 125.18, 125.90, 126.90, 127.36, 127.64, 129.32, 130.80, 131.23, 131.59 ppm.

Synthesis of 1-(1-Pyrenyl)-2-oxodecanethiol, P3. To a stirred solution of **3b** (200 mg, 0.47 mmol) in distilled THF (10 mL), kept at −10 °C, were added hexamethyldisilathiane (102 mg, 0.56 mmol) and 0.6 mL (0.6 mmol) of terabutylammonium fluoride from a 1 M stock solution in THF containing 5% water. The reaction mixture was stirred for 12 h and then diluted with dichloromethane. The organic layer was washed with saturated ammonium chloride solution, and the solvent was removed under reduced pressure. The product was precipitated by adding hexane to give 105 mg (60%) of **P3**, mp 60 °C. IR (KBr), ν_{max}: 2941, 2868, 1142, 850, 724 cm^{-1}. ^1H NMR (300 MHz, $CDCl_3$): δ 1.00−1.29 (12H, m, alkyl), 2.58−2.63 (2H, t, CH_2S), 3.58−3.62 (2H, t, OCH_2), 5.20 (2H, s, $ArCH_2$), 7.97−8.40 (9H, m, aromatic) ppm. ^{13}C NMR (75 MHz, $CDCl_3$): δ 24.96, 28.96,32.52, 33.72, 70.07, 71.57, 123.44, 124.46, 125.18, 125.90, 126.90, 127.36, 127.64, 129.32, 130.80, 131.23, 131.59 ppm. Exact mass calculated 376.1861, (M^+) found 376.1900 (EI^+ high-resolution mass spectroscopy).

Acknowledgment. We thank the Council of Scientific and Industrial Research (CSIR task force project CMM 220239), and the Department of Science and Technology (DST Grant No. SP/S5/NM-75/2002), Government of India for financial support. We also thank Professor P. Natarajan and Dr. P. Ramamurthy, National Centre for Ultrafast Processes, and the Department of Inorganic Chemistry, University of Madras for allowing access to the Picosecond Time Correlated Single Photon Counting and Laser Flash Photolysis facilities. This is contribution No. RRLT-PPD-144 from the Regional Research Laboratory, Trivandrum, India.

Supporting Information Available: Lifetimes of **P1**, **P2**, **P3**, and Au−**P3**; calculation of number of pyrenes and **P2** concentration; FTIR spectra. This material is available free of charge via the Internet at http://pubs.acs.org.

References and Notes

(1) Kamat, P. V. *J. Phys. Chem. B* **2002**, *106*, 7729−7744.
(2) Shipway, A. N.; Katz, E.; Willner, I. *Phys. Chem. Phys* **2000**, *1*, 18−52.
(3) Templeton, A. C.; Wuelfing, W. P.; Murray, R. W. *Acc. Chem. Res.* **2000**, *33*, 27−36.
(4) Imahori, H.; Fukuzumi, S. *Adv. Mater.* **2001**, *13*, 1197−1199.
(5) Shenhar, R.; Rotello, V. M. *Acc. Chem. Res.* **2003**, *36*, 549−561.
(6) Sastry, M.; Rao, M.; Ganesh, K. N. *Acc. Chem. Res.* **2002**, *35*, 847−855.
(7) Thomas, K. G.; Kamat, P. V. *Acc. Chem. Res.* **2003**, *36*, 888−898.
(8) Thomas, K. G.; Ipe, B. I.; Sudeep, P. K. *Pure Appl. Chem.* **2002**, *74*, 1731−1738.
(9) Imahori, H.; Norieda, H.; Yamada, H.; Nishimura, Y.; Yamazaki, I.; Sakata, Y.; Fukuzumi, S. *J. Am. Chem. Soc.* **2001**, *123*, 100−110.
(10) Drexhage, K. H.; Kuhn, H.; Shafer, F. P. *Ber. Bunsen-Ges. Phys. Chem.* **1968**, *72*, 329.
(11) Ipe, B. I.; Thomas, K. G.; Barazzouk, S.; Hotchandani, S.; Kamat, P. V. *J. Phys. Chem. B* **2002**, *106*, 18−21.
(12) Gu, T.; T. Ye; Simon, J. D.; Whitesell, J. K.; Fox, M. A. *J. Phys. Chem. B* **2003**, *107*, 1765−1771.
(13) Gu, T.; Whitesell, J. K.; Fox, M. A. *Chem. Mater.* **2003**, *15*, 1358−1366.
(14) Stellacci, F.; Bauer, C. A.; Meyer-Friedrichsen, T.; Wenseleers, W.; Marder, S. R.; Perry, J. W. *J. Am. Chem. Soc.* **2003**, *125*, 328−329.
(15) Kalyanasundaram, K. *Photochemistry in Microheterogeneous Systems*; Academic Press Inc.: Florida, 1987.
(16) Bricks, J. B. *Photophysics of Aromatic Molecules*; Wiley: London, 1970.
(17) Kalyanasundaram, K.; Thomas, J. K. *J. Am. Chem. Soc.* **1977**, *99*, 2039−2044.
(18) Foster, T. *Angew. Chem., Int. Ed. Engl.* **1969**, *8*, 333.
(19) Bouas-Laurent, H.; Castellan, A.; Desvergne, J.-P.; Lapouyade, R. *Chem. Soc. Rev.* **2001**, *30*, 248.
(20) Hu, J.; Fox, M. A. *J. Org. Chem.* **1999**, *64*, 4959.
(21) Brust, M.; Walker, M.; Bethell, D.; Schffrin, D. J.; Whyman, R. *J. Chem. Soc., Chem. Commun.* **1994**, 801−802.
(22) Hostetler, M. J.; Wingate, J. E.; Zhong, C.-J.; Harris, J. E.; Vachet, R. W.; Clark, M. R.; Londono, J. D.; Green, S. J.; Stokes, J. J.; Wignall, G. D.; Glish, G. L.; Porter, M. D.; Evans, N. D.; Murray, R. W. *Langmuir* **1998**, *14*, 17−30.
(23) Chen, S.; Murray, R. W. *Langmuir* **1999**, *15*, 682−689.
(24) Zhang, J.; Whitesell, J. K.; Fox, M. A. *J. Phys. Chem. B* **2003**, *107*, 6051−6055.
(25) Terill, R. H.; Postlethwaite, T. A.; Chen, C.-h.; Poon, C. D.; Terzis, A.; Chen, A.; Hutchison, J. E.; Clark, M. R.; Wignall, G.; Londono, J. D.; Superfine, R.; Falvo, M.; Johnson, C. S., Jr.; Samulski, E. T.; Murray, R. W. *J. Am. Chem. Soc.* **1995**, *117*, 12537.
(26) Kohlmann, O.; Steinmetz, W. E.; Mao, X.-A.; Wuelfing, W. P.; Templeton, A. C.; Murray, R. W.; Charles S. Johnson, J. C. S. *J. Phys. Chem. B* **2001**, *105*, 8801−8809.
(27) Thomas, K. G.; Zajicek, J.; Kamat, P. V. *Langmuir* **2002**, *18*, 3722−3727.
(28) Alvarez, M. M.; Khoury, J. T.; Schaaff, T. G.; Shafigullin, M. N.; Vezmar, I.; Whetten, R. L. *J. Phys. Chem. B* **1997**, *101*, 3706−12.
(29) Bohre, C. F.; Huffman, D. R. *Absorption and scattering of light by small particles*; Wiley: New York, 1983.
(30) Henglein, A. *Langmuir* **1998**, *14*, 6738−6744.
(31) Thomas, K., G.; Kamat, P. V. *J. Am. Chem. Soc.* **2000**, *122*, 2655−2656.
(32) Chen, M. M. Y.; Katz, A. *Langmuir* **2002**, *18*, 2413−2420.
(33) Chen, M. M. Y.; Katz, A. *Langmuir* **2002**, *18*, 8566−8572.
(34) Shipway, A. N.; Lahav, M.; Willner, I. *Adv. Mater.* **2000**, *12*, 993−998.
(35) Frank, R. S.; Merkle, G.; Gauthier, M. *Macromolecules* **1997**, *30*, 5397.
(36) Cardona, C. M.; Wilkes, T.; Ong, W.; Kaifer, A. E.; McCarley, T. D.; Pandey, S.; Baker, G. A.; Kane, M. N.; Baker, S. N.; Bright, F. V. *J. Phys. Chem. B* **2002**, *106*, 8649.